ISSN (Print) 1226-1750
ISSN (Online) 2233-6656
Journal of Magnetics 28(4), 347-351 (2023) https://doi.org/10.4283/JMAG.2023.28.4.347

Rapid Fabrication of MOD-YIG Films by using Microwave Kiln

Jae-Hyeon An, Eun-Hyuk Kho, Phuoc Cao Van*, and Jong-Ryul Jeong*

Department of Material Science and Engineering, Chungnam National University, Daejeon 34134, Republic of Korea

(Received 2 November 2023, Received in final form 2 November 2023, Accepted 29 November 2023)

Yttrium iron garnet (YIG) is a well-known material extensively utilized in magnonics, spintronics, and spin caloritronics. The development of YIG for practical applications has been the subject of considerable research. In this study, we present the fabrication of YIG films through the thermalization of chemically synthesized YIG using a microwave kiln. The YIG solution was prepared from yttrium and iron precursors in a stoichiometric ratio and subsequently coated onto silicon (Si) substrates. After annealing the coated YIG film with a specific microwave exposure duration, a crystallized YIG film was obtained, confirmed by grazing incidence X-ray diffraction (GI-XRD) analysis. The static magnetic properties were characterized using a vibration sample magnetometer (VSM), revealing comparable parameters, such as coercivity (H_C) = 33.9 ± 0.5 Oe and saturation magnetization (M_S) = 135.9 ± 1.1 emu/cm^3 to those of YIG films annealed using conventional methods, including graphited-based and halogen lamp-based furnaces. Additionally, by using Pt as a spin detection layer, the spin thermoelectric efficiency was investigated via spin Seebeck effect measurements, indicating that YIG films annealed in a microwave kiln exhibit potential as a fabrication technique for YIG applications in spin caloritronics.

Keywords : yttrium iron garnet, microwave kiln, metal-organic decomposition, spin Seebeck effect

1. Introduction

Heterostructures composed of magnetic insulators (MIs) and heavy metals (HMs), exhibiting large spin-to-charge inter-conversion, have drawn considerable attention from researchers due to their fascinating interaction [1-5]. The magnon current can be pumped from MIs into HMs and then converted into electrical charge current which can be used for energy harvesting devices [6]. In contrast, by flowing an electric current in the HMs, the magnetization direction of the MIs layer can be controlled via a so-called spin-orbit torque (SOT) due to the transferring spin angular momentum from the electron in FMs into magnetic moments in the MIs [7, 8]. Moreover, the trilayer configuration of MI/FM/MI has experimentally exhibited the magnon valve effect which can be a noteworthy candidate for substituting the traditional spin valves [9]. The fabrication of HM layers is normally prepared using physical deposition at room temperature [10, 11]. In contrast, the preparation of high-quality MI films requires more careful investigation triggering the attempt on searching for the optimal fabrication approach [12-16].

Undoubtedly, yttrium iron garnet (YIG) stands out as the most popular MI material in the spin-related fields, attributed to its outstanding properties, especially its long-distance spin wave propagation length [17, 18]. Hence there are great efforts in fabricating YIG films which suits to utilize for studying the spin wave behaviors as well as multiple applications [12, 19-23]. The most widely used methods are pulsed laser deposition (PLD), sputtering, and the chemical-based spin coating method. The common features shared by these methods are high-operating or annealing temperatures [12, 13, 18]. Among the available annealing techniques, graphite-based and halogen lamp-based furnaces have gained significant popularity [16, 24-29]. The former is widely used for annealing YIG films at slow or moderate speeds, thus effectively minimizing the effect of thermal shock such as cracks, particularly in cases where there is a significant lattice constant mismatch between the substrate and the film [30-33]. Meanwhile, the latter allows for the rapid preparation of the films, thereby preventing undesired inter-diffusion between the

*Corresponding author: Tel: +82-42-821-6633,
Fax: +82-42-833-3206,
e-mail: caovanphuoc91@gmail.com, jrjeong@cnu.ac.kr

substrate and the film [27, 28]. Nonetheless, it is important to note that both approaches necessitate dedicated designs, and they incur substantial costs.

In this report, for the first time, we demonstrate the facile fabrication of YIG thin film by annealing metal organic decomposition (MOD) spin-coated YIG film in a microwave kiln. We obtained the polycrystalline YIG/Si films of which spin thermoelectric efficiency was also investigated via the spin Seebeck effect (SSE) measurement system.

2. Experimental Procedures

In this study, we used an optimized MOD-YIG solution of which detail can be found in our previous report [13] with 1g-PVP MOD solution condition. Before deposition, the (100)-oriented silicon (Si) substrate was cleaned with acetone and ethanol for 40 minutes each by ultrasonicator. After that, plasma treatment was conducted at 100 watts (W) and 70 kHz for 30 minutes in the argon environment. The MOD solution was then coated onto the substrate using a spin coater. The coated samples were dried in the air on a hot plate set at 100 ºC for 30 minutes. To crystallize the YIG thin films, we employed a microwave oven to supply the heat while the sample was put in a kiln made of SiC which is strongly responsive to microwaves. We conducted the annealing process by placing the kiln with the sample inside a commercial microwave oven with a 600 W output. A 3 nm-thick Pt pattern of 3 × 6 mm was deposited through a shadow mask to measure the SSE voltage. At the two ends of the Pt pattern, Au patterns of 3 mm × 200 μm were deposited and acted as the contact pads.

The crystallinity of each sample was confirmed using high-resolution X-ray diffraction (XRD; Smart Lab model; RIGAKU. Japan). The magnetic properties of the samples were evaluated using a vibrating sample magnetometer (VSM; model 7407; Lake Shore, USA). The morphologies of the samples were assessed using scanning electron microscopy (SEM; CLARA; TESCAN, Czech). The measurement of the SSE voltage was conducted using a homemade system comprising a thermal gradient generated by a commercial strain gauge, with voltage monitored by a Keithley nanovolt meter.

3. Results and Discussion

Initially, we investigated the temperature dependence of the central region of a kiln subjected to microwave irradiation, with the primary objective being the confirmation of the proper functionality of the microwave kiln. The

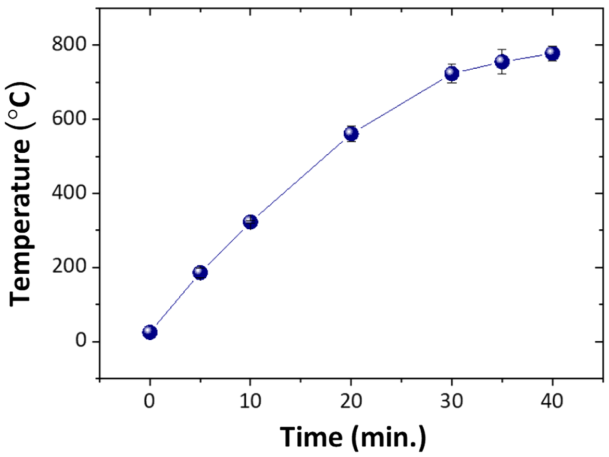

Fig. 1. (Color online) The dependence of temperature inside the kiln on the duration time of applying microwave with power of 600 W.

kiln can strongly interact with the microwave and then convert it into thermal energy. Besides, it has a high melting temperature and low thermal expansion coefficient ensuring the safety and integrity of the annealing process [34]. Real-time temperature monitoring was facilitated through the utilization of a K-type thermocouple constructed from Inconel, which was strategically positioned within the kiln. Fig. 1 illustrates the temperature variation Inside the kiln as a function of microwave exposure duration. It is evident from the data that, within the lower temperature regime, there is a linear temperature increase observed up to a microwave holding time of 20 minutes. Beyond this point, the rate of temperature increment diminishes with prolonged microwave exposure. Notably, after 40 minutes of microwave operation, the temperature attains a level of 778 ± 20 ºC. For context, it is pertinent to reference the crystallization temperature range of YIG, which is typically documented as 700-850 ºC for the annealing process [13, 16, 30, 35-37]. Based on the time-dependent microwave temperature data, we judiciously selected annealing durations of 30, 35, and 40 minutes, all of which are sufficiently prolonged to elevate the temperature above 700 ºC, a crucial requirement for YIG film annealing. To mitigate the potential contamination resulting from the deposition of SiC powder originating from the kiln, a protective quartz cover was employed during the annealing process. Subsequently, we conducted measurements of the static magnetic properties of the fabricated samples under room temperature and ambient atmospheric conditions using a VSM. The results are depicted in Fig. 2. It is noteworthy that only the 40-minute annealing process induced a substantial enhancement in the magnetic moment, while the samples annealed for

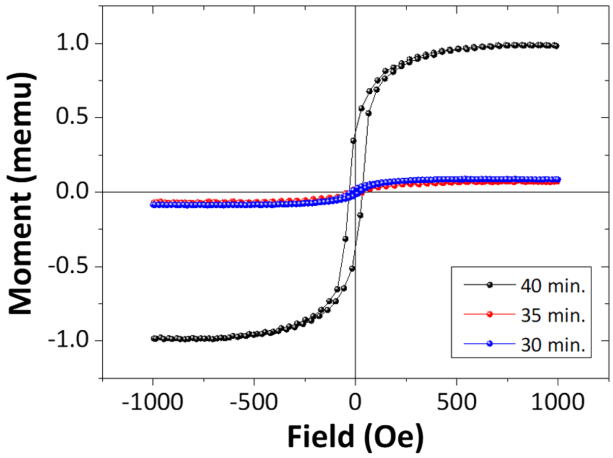

Fig. 2. (Color online) Magnetic hysteresis loops of spin coated films annealed with different duration time of microwave.

30 and 35 minutes exhibited negligible changes. Furthermore, the saturation magnetization (M_S) of this sample measured with the sample subjected to 40 minutes of annealing was evaluated under both in-plane (H_{in}) and out-of-plane (H_{out}) external magnetic field as presented in Fig. 3. The (M_S) and coercivity (H_C) was determined to be 135.9 ± 1.1 emu/cm^3 and 33.9 ± 0.5 Oe, respectively. These findings closely align with the corresponding parameters obtained for bulk YIG and YIG films via conventional annealing processes, as referenced in previous studies [12, 13, 16]. The YIG film has in-plane magnetic anisotropy with the anisotropy field (H_a) ~ 1000 Oe, which is defined as the minimum field to saturate the magnetization along the hard axis. As a minor conclusion, microwave annealing has successfully facilitated the production of YIG films with desirable magnetic properties.

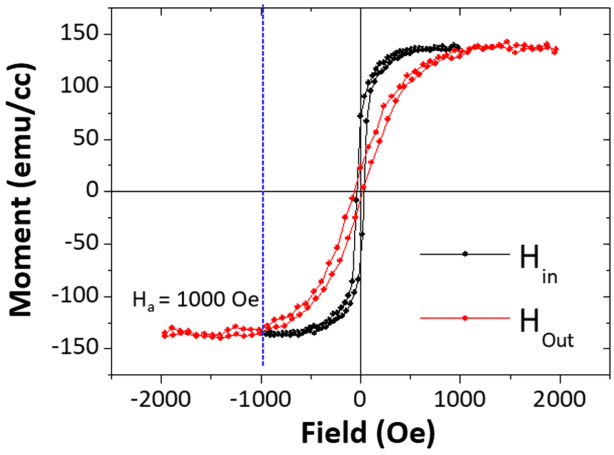

Fig. 3. (Color online) Magnetic properties of 40-minute annealed YIG film.

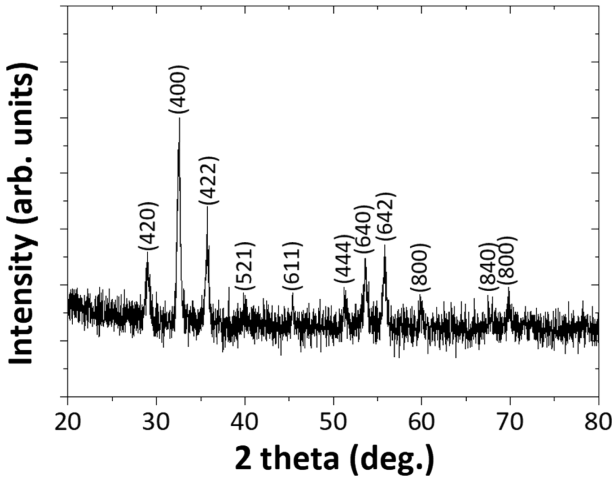

Fig. 4. GI-XRD pattern of 40-minute annealed YIG film.

Moreover, our results suggest that a 35-minute annealing duration falls short of achieving the YIG phase for the MOD spin-coated samples, even when the applied temperature exceeds 700 ºC. Beyond temperature, the holding time during annealing emerges as a critical factor influencing the crystallization of the film.

To ascertain the formation of YIG films and assess their crystallinity, a rigorous investigation was undertaken. Specifically, we conducted a grazing incidence (GI)-XRD analysis on the sample subjected to a 40-minute annealing process. Employing a low incidence angle, we ensured that only signals emanating from the film were captured, as illustrated in Fig. 4. The result shows that our film is poly-crystalline YIG, which is a characteristic configuration when YIG is grown on a Si. Importantly, no discernible peaks corresponding to other phases were observed, thereby affirming the high purity of our YIG film. The (400), (422), and (420) [13, 35, 38] peaks are the preferred orientation of YIG grown on the Si substrate, consistent with the literature, underscoring the reliability and validity of our results.

Surface quality and densification represent crucial parameters for assessing the quality of YIG films. To this end, we examined the surface and cross-sectional morphologies of our YIG sample employing SEM. The results are presented in Fig. 5, with the top and bottom panels displaying surface and cross-sectional images, respectively. The surface analysis reveals the presence of discernible holes within the YIG film. These anomalies can be attributed to the rapid evaporation of solvents during the annealing process. Notably, it is important to emphasize that the temperature exhibited a continuous increase without any pyrolysis processes, contributing to the rapid solvent evaporation and consequent formation of these

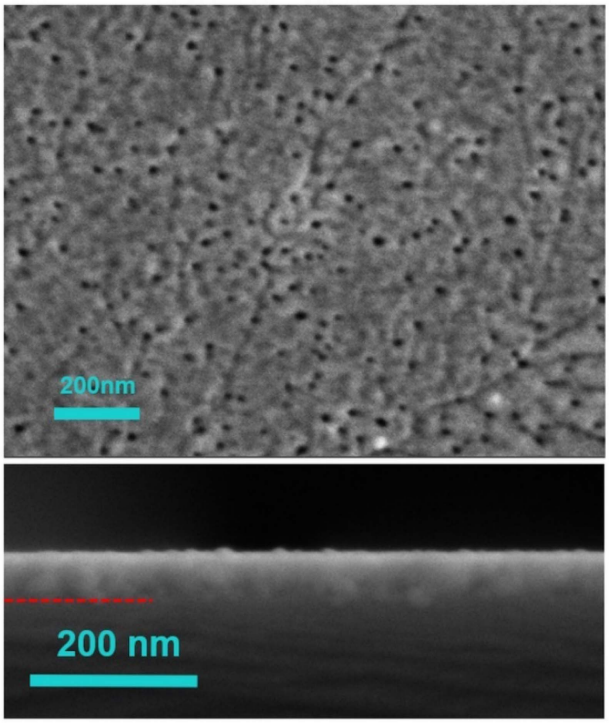

Fig. 5. (Color online) Surface (top image) and cross-sectional (bottom image) morphologies of YIG film annealed in microwave oven for 40 minutes.

holes. Additionally, the observation of cracks can be attributed to the substantial lattice mismatch and variations in thermal expansion coefficients between YIG and the Silicon (Si) substrate [16]. While the resolution of this issue may require a modified annealing procedure, it is imperative to underscore that our primary focus here is to demonstrate the feasibility of YIG film crystallization through microwave annealing. Consequently, we employed the simplest annealing approach for our samples. From the cross-sectional image, we define the thickness of our film as about 47 nm which is used to estimate the saturation magnetization in Fig. 3. Besides, we also can observe the thickness-uniformity of YIG film implying the reliability of the spin coating process.

Spin thermoelectric based on SSE is one of the most important applications of the YIG films. Accordingly, we carried out the SSE measurement and subsequently estimated the spin Seebeck resistivity (SSR) for our YIG sample (40-minute annealed sample). The details of SSE measurements and calculation of SSR can be found in our previous report [39]. Fig. 6 shows the acquired SSR loop, which was obtained while sweeping an external magnetic field, accompanied by a heater power input of 216 mW. It is noteworthy that these loops exhibit analogous behavior to the magnetic hysteresis loop, as measured by the VSM,

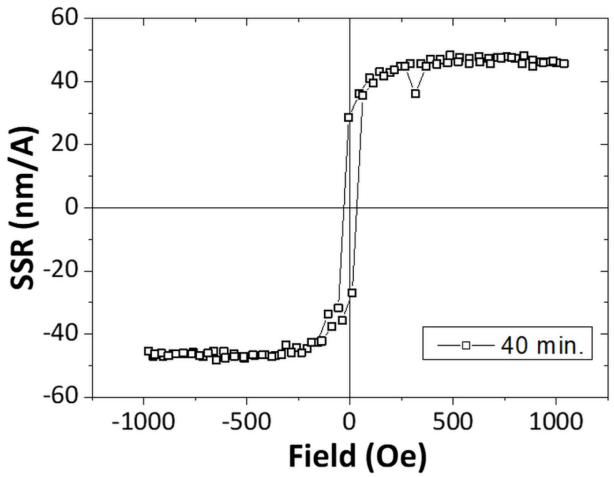

Fig. 6. SSR hysteresis loop of 40-minute annealed YIG film covered by 3 nm-thick Pt.

as the SSE signal is intrinsically linked to the magnetization orientation. Upon exceeding an absolute field magnitude |H| of 500 Oe, corresponding to the sample saturation state, we obtain the maximum SSR value of 46.02 ± 1.45 nm/A. This result aligns with the order of values reported in existing literature [16, 39-41], highlighting the considerable potential of microwave-annealed YIG films for applications in spin thermoelectric devices.

4. Conclusion

In this study, we realized the fabrication of YIG thin films using a commercial microwave oven. We obtain YIG film of which magnetic property is comparable with those annealed by conventional method. The XRD result confirms the crystallinity of YIG, which is polycrystalline with a preferred orientation of (400), (422), and (420) peaks. Furthermore, the SSR value of 46.02 ± 1.45 nm/A is obtained from SSE measurement. Thus, based on this study, there is potential for the introduced annealing method to be considered an effective heat treatment process for fabricating YIG thin films in spintronics.

Acknowledgments

This work was supported by National Research Foundation of Korea (NRF) grant funded by the Korea goverment (No. 2020R1A2C1006136, 2022R1I1A1A 01064438, 2022R1A4A1031349) and BK21 FOUR Program by Chungnam National University Research Grant, 2023. This work was also supported by Samsung Electronics Co. Ltd. (No. SRFCMA2002-02).

References

[1] K. Uchida, J. Xiao, H. Adachi, J. Ohe, S. Takahashi, J. Ieda, T. Ota, Y. Kajiwara, H. Umezawa, H. Kawai, G. E. W. Bauer, S. Maekawa, and E. Saitoh, Nat. Mater. **9**, 894 (2010).

[2] Y. T. Chen, S. Takahashi, H. Nakayama, M. Althammer, S. T. B. Goennenwein, E. Saitoh, and G. E. W. Bauer, Phys. Rev. B **87**, 144411 (2013).

[3] H. L. Wang, C. H. Du, Y. Pu, R. Adur, P. C. Hammel, and F. Y. Yang, Phys. Rev. B. **88**, 100406(R) (2013).

[4] Q. Shao, Y. Liu, G. Yu, S. K. Kim, X. Che, C. Tang, Q. L. He, Y. Tserkovnyak, J. Shi, and K. L. Wang, Nat. Electron. **2**, 182 (2019).

[5] Y. Zhou, C. Guo, C. Wan, X. Chen, X. Zhou, R. Zhang, Y. Gu, R. Chen, H. Wu, X. Han, F. Pan, and C. Song, Phys. Rev. Appl. **13**, 064051 (2020).

[6] A. Kirihara, K. Uchida, Y. Kajiwara, M. Ishida, Y. Nakamura, T. Manako, E. Saitoh, and S. Yorozu, Nat. Mater. **11**, 686 (2012).

[7] C. O. Avci, A. Quindeau, C. F. Pai, M. Mann, L. Caretta, A. S. Tang, M. C. Onbasli, C. A. Ross, and G. S. D. Beach, Nat. Mater. **16**, 309 (2017).

[8] Q. Shao, P. Li, L. Liu, H. Yang, S. Fukami, A. Razavi, H. Wu, K. Wang, F. Freimuth, Y. Mokrousov, M. D. Stiles, S. Emori, A. Hoffmann, J. Åkerman, K. Roy, J.-P. Wang, S.-H. Yang, K. Garello, and W. Zhang, IEEE Trans. Magn. **57**, 1 (2021).

[9] H. Wu, L. Huang, C. Fang, B. S. Yang, C. H. Wan, G. Q. Yu, J. F. Feng, H. X. Wei, and X. F. Han, Phys. Rev. Lett. **120**, 097205 (2018).

[10] J.-M. Kim, C.-Y. Jeon, D.-J. Kim, P. Cao Van, J.-R. Jeong, and B.-G. Park, ACS Appl. Electron. Mater. **2**, 2906 (2020).

[11] J.-M. Kim, D.-J. Kim, C. Cheon, K.-W. Moon, C. Kim, P. Cao Van, J.-R. Jeong, C. Hwang, K.-J. Lee, and B.-G. Park, Nano Lett. **20**, 7803 (2020).

[12] P. Cao Van, S. Surabhi, V. Dongquoc, R. Kuchi, S.-G. S. G. Yoon, and J.-R. Jeong, Appl. Surf. Sci. **435**, 377 (2018).

[13] T. N. Thi, P. C. Van, D. D. Viet, V. D. Quoc, H. Ahn, V. A. Cao, M. G. Kang, J. Nah, B. G. Park, and J. R. Jeong, Ceram. Int. **47**, 16770 (2021).

[14] V. D. Duong, P. Cao Van, T. Nguyen Thi, H. Y. Ahn, V. A. Cao, J. Nah, G. Kim, K.-S. Lee, J.-W. Kim, and J.-R. Jeong, J. Alloys Compd. **927**, 166800 (2022).

[15] P. Cao Van, H. Kim, T. Nguyen Thi, D. Duong Viet, V. A. Cao, J. Nah, S. J. Park, H. Jin, Y. Jo, S.-Y. Park, J. Park, J. M. Yuk, K.-J. Kim, and J.-R. Jeong, J. Alloys Compd. **941** (2023) 169019.

[16] J.-H. Seol, J.-H. An, G.-W. Park, T. Nguyen Thi, D. Duong Viet, B.-G. Park, P. C. Van, and J.-R. Jeong, Thin Solid Films **774**, 139846 (2023).

[17] L. J. Cornelissen, J. Liu, R. A. Duine, J. Ben Youssef, and B. J. van Wees, Nat. Phys. **11**, 1022 (2015).

[18] G. Schmidt, C. Hauser, P. Trempler, M. Paleschke, and E. Th. Papaioannou, Physica Status Solidi (b). **257**, 1900644 (2020).

[19] C. Safranski, I. Barsukov, H. K. Lee, T. Schneider, A. A. Jara, A. Smith, H. Chang, K. Lenz, J. Lindner, Y. Tserkovnyak, M. Wu, and I. N. Krivorotov, Nat. Commun. **8**, 117 (2017).

[20] Z. Li, X. Zhang, D. Zhang, B. Liu, H. Meng, J. Xu, Z. Zhong, X. Tang, H. Zhang, and L. Jin, APL Mater. **10**, 021101 (2022).

[21] M. S. Sarker, H. Yamahara, L. Yao, S. Tang, Z. Liao, M. Seki, and H. Tabata, Sci. Rep. **12**, 11105 (2022).

[22] P. Cao Van, T. T. Nguyen, V. D. Duong, M. H. Nguyen, J.-H. Seol, G.-W. Park, and J.-R. Jeong, Curr. Appl. Phys. **42**, 80 (2022).

[23] S. Guo, B. McCullian, P. Chris Hammel, and F. Yang, J. Magn. Magn. Mater. **562**, 169795 (2022).

[24] H. Buhay, J. D. Adam, M. R. Daniel, N. J. Doyle, M. C. Driver, G. W. Eldridge, M. H. Hanes, R. L. Messham, and M. M. Sopira, IEEE Trans. Magn. **31**, 3832 (1995).

[25] S. Li, W. Zhang, J. Ding, J. E. Pearson, V. Novosad, and A. Hoffmann, Nanoscale **8**, 388 (2016).

[26] S.-Y. Sung, X. Qi, S. K. Mondal, and B. J. H. Stadler, MRS Online Proceedings Library (OPL) **817** L8.3. (2004).

[27] M. Aldosary, J. Li, C. Tang, Y. Xu, J.-G. Zheng, K. N. Bozhilov, and J. Shi, Appl. Phys. Lett. **108**, 242401 (2016).

[28] T. Nozue, T. Kikkawa, T. Watamura, T. Niizeki, R. Ramos, E. Saitoh, and H. Murakami, Appl. Phys. Lett. **113**, 262402 (2018).

[29] H. Bai, X. Z. Zhan, G. Li, J. Su, Z. Z. Zhu, Y. Zhang, T. Zhu, and J. W. Cai, Appl. Phys. Lett. **115**, 182401 (2019).

[30] X. Guo, Y. Chen, G. Wang, Y. Zhang, J. Ge, X. Tang, F. Ponchel, D. Rémiens, and X. Dong, J. Alloys Compd. **671**, 234 (2016).

[31] J. Lian, Y. Chen, Z. Liu, M. Zhu, G. Wang, W. Zhang, and X. Dong, Ceram. Int. **43**, 7477 (2017).

[32] K. Li, H. Zheng, P. Zheng, J. Xu, J. Chen, J. Zhou, and L. Zheng, Mater. Lett. **228**, 21(2018).

[33] R. Xiang, L. Chen, S. Zhang, H. Li, J. Du, Y. W. Du, and R. H. Liu, Mater. Res. Express. **7**, 046105 (2020).

[34] D. Obermayer, B. Gutmann, and C. O. Kappe, Angew. Chem. **121**, 8471 (2009).

[35] X. Guo, Y. Chen, G. Wang, Y. Zhang, J. Ge, X. Tang, F. Ponchel, D. Rémiens, and X. Dong, J. Am. Ceram. Soc. **99**, 2217 (2016).

[36] M. A. Musa, R. S. Azis, N. H. Osman, J. Hassan, and T. Zangina, Results Phys. **7**, 1135 (2017).

[37] I. Lucas, P. Jiménez-Cavero, J. M. Vila-Fungueiriño, C. Magén, S. Sangiao, J. M. de Teresa, L. Morellón, and F. Rivadulla, Phys. Rev. Mater. **1**, 74407 (2017).

[38] L. K. C. S. Assis, J. E. Abrão, A. S. Carvalho, L. A. P. Gonçalves, A. Galembeck, and E. Padrón-Hernández, J. Magn. Magn. Mater. **568**, 170388 (2023).

[39] P. C. Van, D. D. Viet, T. N. Thi, J.-H. Seol, G.-W. Park, and J.-R. Jeong, J. Magn. **27**, 1 (2022).

[40] A. Prakash, B. Flebus, J. Brangham, F. Yang, Y. Tserkovnyak, and J. P. Heremans, Phys. Rev. B. **97**, 020408(R) (2018).

[41] G. Venkat, T. A. Rose, C. D. W. Cox, G. B. G. Stenning, A. J. Caruana, and K. Morrison, EPL **126**, 37001 (2019).